MAPPING LAND USE LAND COVER OF TRA VINH PROVINCE IN 2020 USING MULTI-TEMPORAL AND MULTI-SOURCE OF REMOTE SENSING IMAGERY

Thi Hong Diep Nguyen[1], Duy Tien Pham[2], Kieu Diem Phan[1], Thi Cam Nhung Dinh[1], Thanh Tran Giam[1]
[1]Can Tho University, Campus II, 3/2 street, Ninh Kieu district, Can Tho 900000, Viet Nam,
Emai: (nthdiep, pkdiem)@ctu.edu.vn; dtcnhung20@gmail.com; thanhgiam102@gmail.com
[2]An Giang University, No. 18, Ung Van Khiem street, Dong Xuyen ward, Long Xuyen city, An Giang 880000, Viet Nam, Email: pdtien.agu@gmail.com

KEYWORDS: SENTINEL-1A, LANDSAT, MODIS, Object-Based Image Analysis (OBIA), Random Forest (RF).

ABSTRACT: This research discusses a methodology to create a Land Use Land Cover (LULC) map in the Tra Vinh province, using MODIS, LANDSAT 8 OLI, and SENTINEL-1A imagery in 2020. The MODIS MOD09A1 8-day composite products were processed NDVI maps and then classified LULC types using the ISODATA algorithm in unsupervised classification. The Normalized Difference Water Index (NDWI), Normalized Difference Built-up Index (NDBI), Normalized Difference Vegetation Index (NDVI), and brightness value extracted from LANDSAT 8 OLI were applied to map locally common LULC types using the Object-Based Image Analysis (OBIA) method. SENTINEL-1A was used to remove the threshold backscatter values for the performance of two commonly used classifiers of Support Vector Machine (SVM) and Random Forest (RF) for land use classification. The accuracy of the LULC map was evaluated for nine classes including triple-rice, double-rice crops, perennial/orchards, aquaculture, shrimp-single rice crop rotation, build-up area, upland crop, mangrove forest, and rivers/canals. In which rice crops (triple-rice crop and double-rice crop) and perennial/orchards areas occupied the greatest extent, approximately 44,36% and 19,39% of total natural area, respectively. The archived LULC map was also compared to geospatial reference data and local inventory statistics data. The accuracy of the LULC map could be improved by combining different classifiers with an overall accuracy at 87±1.5% and Kappa coefficient at 0.77±0.2 and a difference of about ±5% compared to the local inventory statistics data. This study has indicated the potential performance of integrated different sensors in mapping LULC. The strengthened understanding of multiple resource imagery provides better results in updating details of agriculture land use maps on a regional scale.

1. INTRODUCTION

Satellite images provide a wide range of detecting the natural resources and environment possibilities in a fast way, especially the areas are unavailable for a field survey based on the topography, dense vegetation, or other local factors (Schowengerdt, 2007; Van Dessel et al., 2008; Lóki-Szabó, 2011; Burai et al., 2014; Varga et al., 2015). There are many earth observation satellites that have different types of spatial and spectral resolutions used in these analyses (Singh et al., 2014; Srivastava et al., 2015). Therefore, the authors have to consider different satellite images to develop the mapping aims to determine the scale of the investigation for any purposes (Berke et al., 2013; Deák et al., 2013). Land cover mapping by satellite images used several algorithms of classification as Minimum Distance (Davies 2004), Maximum Likelihood (Wernick-Morris, 1988), Support Vector Machine, Random Forest (Jin et al., 2005; Otukei-Blaschke, 2010), etc., providing an acceptable thematic error for mapping. Another way of the application using the images is spectral features as all surface objects have a given specific spectral profile to be used it to determine measurable quantities (Kovács-Szabó, 2016). However, a spectral band alone rarely corresponds with a quantifiable amount, thus band ratios are often used in remote sensing studies. The first published band ratio, the Normalized Difference vegetation Index (NDVI), became a favored tool of biomass estimation (Rousse et al., 1973). Many indices were developed for different purposes to identify, e.g., water bodies (NDWI, McFeeters, 1996), bare lands (BI, Zhao, and Chen, 2005; NDBal, Chen, 2006). Besides, monitoring the restoration of the overall objective of this study is to evaluate the utility of LANDSAT, MODIS, and SENTINEL-1A multi-spectral data for land cover classification in Tra Vinh province, Vietnam. The second objective is to compare the pixel-based and non-parametric RF classification methods concerning overall and class-level accuracy.

2. METHODS

2.1. Data Collection

+ LANDSAT 8 OLI data: We used LANDSAT 8 OLI images freely available from the LANDSAT archives (https://earthexplorer.usgs.gov/). The spatial resolution of the LANDSAT OLI sensors is 30m for the bands 1-7 and 9, and 15m for the panchromatic band (band 8), and 100m for thermal bands (band 10 and 11).

+ MODIS data: the MODIS data used is the standard 8-day composite surface reflectance MODIS image dataset of the LP DAAC centre, acquired from the AQUA satellite and processed to level 3 (data name is MOD09Q1). For this level, the MODIS data has been preliminarily filtered by NASA's algorithm and selected the best monitoring results for eight time series sequences for each image cell (pixel). Each image consists of 2 bands (band 1 - red-wave spectrum with a spectral centre of 645 nm and band 2 - near-infrared range with a spectral centre of 858 nm) at a spatial resolution of 250 m and has been returned to the global Sinusoidal coordinate system.

+ SENTINEL-1A data: downloading from the European Space Agency (ESA) Copernicus website at: https://scihub.copernicus.eu/dhus/#/home. SENTINEL-1A active remote sensing image includes VV and VH polarization, wideband interference (IW) scanning mode with a scan width of 250 km, the spatial resolution of 5x20 m. Furthermore, level 1 processing level GRD (Ground Range Detected), 10x10 m pixel size, gives more ground polyhedron images than SLC (Single Look Complex).

2.2. Study Area Extract

SENTINEL-1A image in wideband interference scanning mode has a scanning width of 250 km, LANDSAT image 185 km, MODIS image 2,330 km, the image covers the entire large area. Therefore, extracting the research area is essential to save processing time as well as reduce storage capacity.

2.3. Atmospheric Correction

The sensor receiving the electromagnetic radiation is influenced by the atmosphere. The purpose of the atmospheric correction is to remove the effects of the atmosphere on the image data and produce a reflectance value of actual radiation from the ground (Reflectance value). The reflectance value from bands 1 to 7 of the LANDSAT image is calculated based on the Dark Object Subtraction (DOS) tool.

2.4. Data Analysis

2.4.1. LANDSAT Data

We concentrated on synthesizing and independently investigating several features using the supervised object-based image classification process for land-cover including: (1) spatial resolution of images used; (2) segmentation methods or scale; (3) training sample data sets; (4) imagery indices (5) supervised classification; and (5) study types or the number of classified categories. These measures were calculated into a essential measurement and a specific standard deviation conditions to analyse each factor's effect. A particular sensor and a specific supervised classifier were used to assess the impact size from these various factors. In addition, the correlation between spatial resolution of the image used can determine the characteristics of the study area or segmentation scale was reported.

We extracted and analysed measures of overall accuracy from the individual case studies. The comparison results were used to assess the effect from classifiers from the mean overall accuracies of classifiers. In addition, the classification process provided coherent guidance on the relative performance of different features to disclose ways for improving classification accuracy by controlling these uncertain factors.

2.4.3. MODIS Data

NASA (National Aeronautics and Space Administration) acquired the MODIS imagery website (http://ladsweb.nascom.nasa.gov/); specifically, the surface reflectance MOD09A1 eight-day composite products. We applied the first two bands of the MOD09A1 data for NDVI index images and the corresponding Quality Assessment (QA) data. NDVI data facilitate meaningful comparisons on seasonal and inter-annual changes in vegetation growth and activity for detecting rice from time-series MODIS data. The method includes two major procedures: (i) building a standard NDVI time-series base on rice growth cycles through field sampling data; and (ii) extracting rice fields due to the standard rice-growth NDVI time-series data.

2.4.3. SENTINEL-1A Data

The study used the SNAP and EnMAP Box software Classifier Vector Machine (SVM) and Random Forest (SVM) to classify Sentinel 1A images. Two parameters must be defined in the RF classifier to create a predictive model:

the number of desired trees classifier k and the predictive features number m used in each subdivision to grow the tree (Rodriguez Galiano et al., 2012). In this study, k was set to 100, and the number of predictive characteristics m was set to the square root of all features to generate an RF classifier (Eisavi et al., 2015).

The SVM algorithm separates data training samples based on optimal hyperplanes which separates the data into classes, positioning decision boundaries to minimize classification errors between types (Fukuda et al., 2002). SVM classification requires the selection of a kernel function. The study used the Gaussian Radial Basis Function (RBF) kernel (Lardeux et al., 2009; Trisasongko et al., 2017). We used a grid search method with predefined intervals that proved effective (van der Linden et al., 2015).

2.5 Accuracy Assessment

The accuracy assessment evaluate the images classification results, the reference sampling locations were selected a complete variety of LULC classes across the entire study area. Three hundred two locations were extracted based on the stratified random sampling procedure described by Stehman (1999). Class decisions were observing based on an area around the sampling location. Also, an error matrix was identified comparing between land cover classifications on the map and the ground-truth categories. The extent of these two classifications levels was defined as the map accuracy according to Congalton's (1991) procedure.

3. RESULTS

Based on the formula for estimating the survey points of Corchan (1977), the research has tested a total of 302 points. The test points are distributed at different status types, depending on the percentage of the area analyzed for each land use on the map. The overall accuracy of the classification results was 88.7%, and the Kappa coefficient = 0.77 (LANDSAT-MODIS imagery); overall accuracy was 85%, and the Kappa coefficient = 0.77 (SENTINEL-1A). From this result, the accuracy of classification results is satisfactory (specified more than 85%), and the classification ability has good reliability (Kappa ≥ 0.70).

The study area's land uses were categorized into the following ten groups including (1) Double rice crop, (2) Triple rice crop, (3) Perennial/orchards, (4) Built-up, (5) Water, (6) Upland crop, (7) Forest, (8) Aquaculture, (9) Shrimp-rice rotation and forest-shrimp combination (Figure 1). The triple-rice crop and perennial plant/orchards covered the highest area at 37.95% and 21.62 %. On the other hand, the following land use types of aquaculture, double-rice crop, and river were high in distribution at 16.39%, 11.51%, and 10.34%, respectively. The remaining land use types area (build-up and forest-shrimp combination) were distributed lower than 7% of the total area. The last land-use types (rice-shrimp rotation, forest, and upland crop) were single rice crop and urban area with the distribution area at 0.65% and 0.69%, respectively.

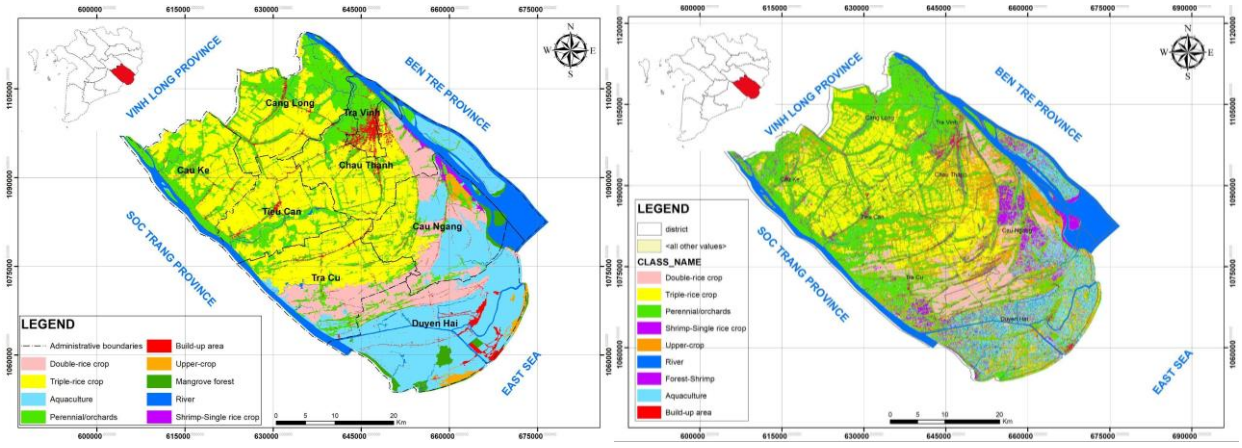

(a) (b)

Figure 1. Land Use Land Cover Map in 2020 (a) LANDSAT and MODIS Image Series, (b) SENTINEL-1A

Among the eight districts/towns in Tra Vinh province, three sections covered almost nine land-use types, including Cau Ngang, Chau Thanh, and Duyen Hai. The distributed except Duyen Hai district has no triple-rice crops cultivation regarding to Duyen Hai district's geographical position in the coastal area that were regularly affected by the saline intrusion. The remaining five sections, including Cang Long, Cau Ke, Tieu Can, Tra Cu, and Tra Vinh,

cover five land-use types: triple-rice crop, perennial/orchards, and aquaculture, and build-up areas. These districts are distributed inland, so they cultivate mainly crops belonging to freshwater ecosystems.

Regarding statistics data for land inventory in Tra Vinh province in 2020, land use area based on classification has a difference between LANDSAT-MODIS (MOD09) images and SENTINEL-1A image classification with less than 10% and 20%, respectively in which the highest difference mentioned on rice crop and upland crop on SENTINEL-1A. However, total differences for both imagery have a similar difference at 6.65% and 6.96%. However, the area in land inventory statistics data has a difference of around 25,000 ha (6.23%) because of the different techniques to estimate land-use area.

Table 1. Comparison LULC classified by multi-sources imagery in Tra Vinh province.

LULC	Statistics data	LANDSAT-MODIS MOD09		SENTINEL-1A	
		Area (ha)	Percentage (%)	Area (ha)	Percentage (%)
Rice	82,743.05	103,194.87	-9.38	43,856.09	17.83
Aquaculture	36,563.60	49,435.38	-5.90	32,949.91	1.66
River	24,268.12	21,568.93	1.24	32,516.46	-3.78
Perennial/Orchards	48,771.91	45,099.67	1.68	33,485.71	7.01
Upper-crop	9,972.53	1,402.80	3.93	51,618.48	-19.09
Build-up area	8,939.21	8,624.93	0.14	28,535.03	-8.98
Forest	6,861.86	3,297.21	1.63	10,346.55	-1.60
Total	218,120.28	232,623.79	6.65	233,308.23	6.96

4. DISCUSSION

The study attempted to apply an satellite data to different classification tasks. A highly detailed reference database was more complex with ten possible land cover classes and several fundamental landscape indicators by using image indices. Prior research showed the effectiveness of object-based image analysis of high-resolution images (Ma, L et al., 2017). Segmentation forms the object-based image analysis (OBIA) basis and creates small homogeneous objects from LANDSAT images (Blaschke, T et al., 2000). Even though this method has also been used on medium-resolution imagery, the goal is to examine an area of interest at larger scales and obtain information about an image's texture. Regarding to the results of previous research (Narumalani, S et al., 1998; Blaschke, T et al., 2000; Aguirre-Gutiérrez, J et al., 2012; Senthilnath, J. et al., 2012; Zanotta, D.C et al., 2018), the applicability of segmentation has been demonstrated in the land cover classification of medium-resolution satellite images. Although only pixel-based variety was performed, segmentation could improve the accuracy of the classified images compared to spectral values independent of the minimal segment size or the area's fragmentation rate.
These results indicated that more research needs to be conducted using other reference data (Land Use and Coverage Area Survey point-LUCAS point) and reference points from high-resolution satellite imagery or field survey data. For example, we can examine the impact of a reference's Manchester Metropolitan University (MMU) and the importance of the reference data's reliability; we can determine the different use of the LANDSAT and SENTINEL imagery data source is better for our study. Otherwise, a future step is to combine the use of different scales and to apply other more sophisticated metrics that describe the landscape structure.

5. CONCLUSION

We developed a method for remote-sensing LULC detection that uses multi-temporal high-resolution imagery. The technique applies an object-based, supervised classification and support vector machine (SVM) algorithm approach using geostatistical features obtained as input data. The accuracy of the classification was consistently high. The accuracy of land classification is crucial to identify the characteristics of the land and make reasonable use of land

resources. The areas with the most incredible intensity of LULC in Tra Vinh are concentration in the triple-rice crop, aquaculture, and perennial plant/orchards.

Acknowledgment

We highly appreciate being funded in part by the Technological Cooperation Project of Jica's Building capacity for Can Tho University to be an excellent institution of education, scientific research, and technology transfer. We are also grateful to the Can Tho University Improvement Project VN14–P6, funded by the Japanese ODA loan, and to all those who provided us the possibility to complete this research through the ODA-E8 project.

References

Aguirre-Gutiérrez, J., Seijmonsbergen, A.C., Duivenvoorden, J.F., 2012. Optimizing land cover classification accuracy for change detection, a combined pixel-based and object-based approach in a mountainous area in Mexico. Appl. Geogr., 34, pp. 29-37.

Blaschke, T., Lang, S., Lorup, E., Strobl, J., Zeil, P., 2000. Object-Oriented Image Processing in an Integrated GIS/Remote Sensing Environment and Perspectives for Environmental Applications. In: Cremers, A. B. & Greve, K. (Hrsg.), Umweltinformatik ’00 Umweltinformation für Planung, Politik und Öffentlichkeit. Marburg: Metropolis.

Berke, J., Bíró, T., Burai, P., Kováts, L.D., KozmaBognár, V., Nagy, T., Tomor, T., Németh, T., 2013. Application of remote sensing in the redmud environmental disaster in Hungary. Carpathian Journal of Earth and Environmental, 8, pp. 49-54.

Blaschke, T., 2010. Object based image analysis for remote sensing. ISPRS J. Photogramm. Remote Sens., 65, pp. 2-16.

Burai, P., Deák, B., Valkó, O., Lénárt, Cs., 2014. Mapping of Grass Species Using Airborne Hyperspectral Data. In: Pfeifer, N. Zlinszky, A. (Eds.): Proceedings of the International Workshop on Remote Sensing and GIS for Monitoring of Habitat Quality, Vienna, Austria, University of Technology, pp. 87-88.

Chen, X.L., Zhao, H.M., Li, P.X., Yin, Z.Y., 2006. Remote sensing image-based analysis of the relationship between urban heat island and land use/cover changes. Remote Sensing of Environment, 104, pp. 133-146.

Cochran, W.G., 1977. Sampling Techniques. 3rd Edition, John Wiley & Sons, New York.

Congalton, 1991. A review of assessing the accuracy of classifications of remotely sensed data. Remote Sensing of Environment, 37 (1), pp. 35-46.

Davies, E.R., 2004. Machine Vision: Theory, Algorithms and Practicalities, Third Edition, Elsevier, San Fransisco.

Deák, M., Telbisz, T., Árvai, M., Mari, L., Horváth, F., 2013. Subpixel Vegetation Classification of EO-1 Hyperion Data Through Spectral Reduction, A Case Study in Hungary. In: He Yingbin, Gao Mingjie, Zhou Zhenya (Eds.) (2013): The Application of Remote Sensing and GIS Technology in Crop Production. Beijing, 2013.08.26-2013.08.30. China, Agricultural Science and Technology Press (CASTP), pp. 83–88.

Eisavi, V., Homayouni, S., Maleknezhad Yazdi, A., Alimohammadi A., 2015. Land cover mapping based on random forest classification of multitemporal spectral and thermal images. Environmental Monitoring and Assessment, 187 (291), pp. 187-291.

Fukuda, Y., Aoki, S., and Doi, K., 2002. Impact of satellite gravity missions on glaciology and Antarctic Earth sciences. Polar Meteorology and Glaciology, 16, pp. 32-41.

Greg, E. LAADS Web, Retrieved December 25, 2020, from http://ladsweb.nascom.nasa.gov/.

Jin, S., Li, D., Wang, J., 2005. A comparison of support vector machine with maximum likelihood classification algorithms on texture features. Proceedings. IEEE International Geoscience and Remote Sensing Symposium, 5, pp. 3717-3720.

Kovács, Z., Szabó, Sz., 2016. An interactive tool for semi-automated feature extraction of hyperspectral data. Open Geosciences, 8, pp. 493-502.

Lardeux, C., Frison, P.L., Tison, C., Souyris, J.C., Stoll, B., Fruneau, B., and Rudan, J.P., 2009. Support vector machine for multifrequency SAR polarimetric data classification, IEEE Trans. Geosci. Remote Sens., 47 (12), pp. 4143-4152.

Lóki, J., Szabó, J., 2011. Changes of the forests of "Nagyerdő" in Debrecen with remote sensing techniques. Nyíregyháza: Nyíregyházi Főiskola Turizmus és Földrajztudományi Intézet, pp. 309-321.

Ma, L., Li, M., Ma, X., Cheng, L., Du, P., Liu, Y., 2017. A review of supervised object-based land-cover image classification. ISPRS J. Photogramm. Remote Sens., 130, pp. 277-293.

Mcfeeters, S. K., 1996. The use of the Normalized Difference Water Index (NDWI) in the delineation of open water features. International Journal of Remote Sensing, 17 (7), pp. 1425-1432.

Narumalani, S., Zhou, Y., Jelinski, D.E., 1998. Utilizing geometric attributes of spatial information to improve digital image classification. Remote Sens. Rev., 16, pp. 233–253.

Otukei, J.R., Blaschke, T., 2010. Land cover change assessment using decision trees, support vector machines and maximum likelihood classification algorithms. International Journal of Applied Earth Observation and Geoinformation, 12 (1), pp. 27-31.

Rodriguez Galiano, V.F., 2012, Ghimire, B., Rogan J., Chica-Olmo, M., Rigol-Sanchez, J.P., 2012. An assessment of the effectiveness of a random forest classifier for land-cover classification. ISPRS J. Photogramm. Remote Sens., 67 (1), pp. 93-104.

Rouse, J.W., Haas, R.H., Schell, J.A., Deering, D.W., 1973. Monitoring vegetation systems in the great plains with ERTS. Third 80 ERTS Symposium, NASA SP-351, pp. 309-317.

Stehman, 1999. Basic probability sampling designs for thematic map accuracy assessment. J. Remote Sens., 20, pp. 2423-2441.

Schowengerdt, R.A., 2007. Remote Sensing, Third Edition: Models and Methods for Image Processing. Elsevier, Arizona.

Senthilnath, J., Bajpai, S., Omkar, S., Diwakar, P., Mani, V., 2012. An approach to multi-temporal MODIS image analysis using image classification and segmentation. Adv. Space Res., 50, pp. 1274-1287.

Singh, S.K., Pandey, A.C., Singh, D., 2014. Land Use Fragmentation Analysis Using Remote Sensing and Fragstats. Remote Sensing Applications in Environmental Research, Series Society of Earth Scientists Series, pp. 151-176.

Stehman, S.V., 1999. Basic probability sampling designs for thematic map accuracy assessment. International Journal of Remote Sensing, 20 (12), pp. 2423-2441.

Trisasongko, H., Panuju, R., David, J.P., Xiuping, J., Griffin L., 2017. Comparing six pixel-wise classifiers for tropical rural land cover mapping using four forms of fully polarimetric SAR data. International Journal of Remote Sensing, 38 (11), pp. 3274-3293.

Van Dessel, W., Van Rompaey, A., Poelmans, L., Szilassi, P., 2008. Predicting land cover changes and their impact on the sediment influx in the Lake Balaton catchment. Landscape Ecology, 23 (6), pp. 645-656.

Varga, Z., Czedli, H., Kezi, C., Lóki, J., Fekete, Á., Biro, J., 2015. Evaluating the Accuracy of Orthophotos and Satellite Images in the Context of Road Centerlines in Test Sites in Hungary. Research Journal of Applied Sciences, 10, pp. 568-573.

Wernick, M., Morris, G. M., 1988. Maximum-Likelihood Image Classification. Proc. SPIE 0938, Digital and Optical Shape Representation and Pattern Recognition. https://doi.org/10.1117/12.976607.

Zanotta, D.C., Zortea, M., Ferreira, M.P., 2018. A supervised approach for simultaneous segmentation and classification of remote sensing images. ISPRS J. Photogramm. Remote Sens., 142, pp. 162-173.

Zhao, H., Chen, X., 2005. Use of normalized difference bareness index in quickly mapping bare areas from TM/ETM+. Geoscience and Remote Sensing Symposium. Proceedings. IEEE International, 3, pp. 1666-1668.